ELSEVIER

Journal of Organometallic Chemistry 626 (2001) 24–31

Journal of Organometallic Chemistry

www.elsevier.nl/locate/jorganchem

Entropy effects in gas phase ion-molecule association reactions

Giuseppe Innorta [a,*1], Sandro Torroni [a], Andrea Maranzana [b], Glauco Tonachini [b,*2]

[a] *Dipartimento di Chimica 'Giacomo Ciamician', Università di Bologna, via Selmi n. 2, I-40126 Bologna, Italy*
[b] *Dipartimento di Chimica Generale e Organica Applicata, Università di Torino, Corso Massimo D'Azeglio 48, I-10125 Torino, Italy*

Received 25 September 2000; received in revised form 7 December 2000

Abstract

The kinetics of gas phase reactions of the ions $C_5H_5M^+$ (M = V, Co, Ni and Ru) with oxygen (Me_2CO, Me_2O, MeOH, Me_2CHOH, H_2O) and nitrogen (NH_3, NH_2Me, $NHMe_2$, NMe_3) donor ligands have been studied by Ion Trap Mass Spectrometry. The kinetic data confirm the previously found dependence of the log of the rate constants upon the ligand ionization energy. To get some insight on the origin of the existing barrier to the reaction some experiments were performed at various temperatures; it was found that the kinetic constants increased when the temperature decreased. The results are compatible with an entropy effect on the free energy of activation as also shown by some calculations performed for the reaction of the $C_5H_5Fe^+$ ion with water.

Keywords: Gas-phase chemistry; Ion-molecule reactions; Kinetics; Mass spectrometry; Metallocenes

1. Introduction

The gas phase reactions between a metal containing ion and a neutral molecule can occur with a wide range of efficiencies. While a low efficiency can be sometimes justified on the ground of either the electronic structure of the metal ion [1] or the reaction mechanism [2], there are several cases, especially in association reactions, for which the reasons for low efficiency have not been ascertained. In a previous paper [3] we reported that the ion $C_5H_5Fe^+$ reacts with small ligands by forming association products, and that the rate constants of its reactions are influenced by the ionization energy of the ligands. We now extend this study to other $C_5H_5M^+$ ions.

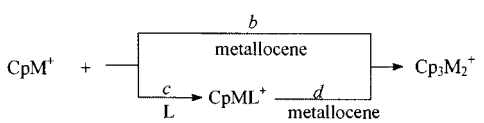

Scheme 1. Reaction sequence of the ion $C_5H_5M^+$ with gaseous ligands. Where *b*, *c* and *d* are the kinetic constants.

2. Results and discussion

2.1. The reactions

As already found with the ferrocene, the reactions of the ions $C_5H_5M^+$ in the ITMS in the presence of a ligand lead to a variety of products. Formation of $(C_5H_5)_2M^+$ and especially of $(C_5H_5)_3M_2^+$ is always observed, but at low metallocene pressure in the ion source these reactions are minimized; it was possible in most cases to avoid the charge exchange reaction. The reactions with the ligands L lead usually to the formation of the corresponding adduct ions $C_5H_5ML^+$. In a few cases, ions obtained by loss of small neutrals from the adduct ions are also present.

The general reaction scheme in the adopted experimental conditions is reported in Scheme 1.

2.2. The kinetics

In the present experimental conditions, the disappearance of the ion $C_5H_5M^+$ must follow first order kinetics as was found in all cases, so that a pseudo first order rate constant can be obtained from the semi-log plot of the relative abundance of the ion $C_5H_5M^+$ versus time. However it was necessary to use a quite

[1] *Corresponding author. E-mail: innorta@ciam.unibo.it.
[2] *Corresponding author. E-mail: tonachini@ch.unito.it

0022-328X/01/$ - see front matter
PII: S0022-328X(00)00945-1

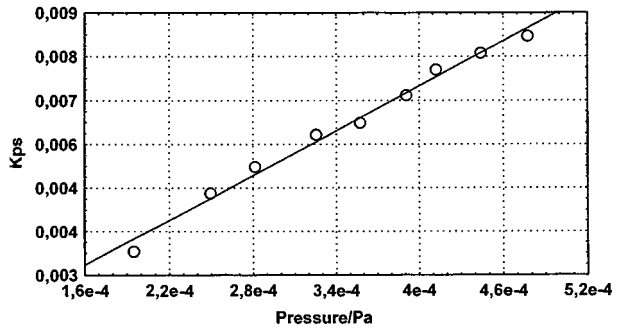

Fig. 1. Pseudo first order rate constant for the reaction of $C_5H_5Ni^+$ with NH_3 vs. ammonia pressure.

Table 1
Kinetic data for the reactions of the ion $C_5H_5Co^+$

Molecule	$k_1 \times 10^9$ [a]	$k_c \times 10^9$ [b]	k_1/k_c
$(CH_3)_2CO$	1.99 ± 0.0435	2.06	0.969
$(CH_3)_2O$	0.764 ± 0.0264	1.30	0.586
$CH_3CH(OH)CH_3$	0.933 ± 0.0573	1.46	0.638
CH_3OH	0.291 ± 0.018	1.61	0.180
H_2O	0.0287 ± 0.0029	1.95	0.0144
$(CH_3)_3N$	1.30 ± 0.0626	1.22	1.07
$(CH_3)_2NH$	1.02 ± 0.0448	1.29	0.789
CH_3NH_2	0.966 ± 0.149	1.48	0.654
NH_3	0.439 ± 0.0138	1.80	0.249

[a] Rate constants are expressed in cm^3 $molecule^{-1}$ s^{-1}.
[b] Calculated according to Ref. [4].

Table 2
Kinetic data for the reactions of the ion $C_5H_5Ni^+$

Molecule	$k_1 \times 10^9$ [a]	$k_c \times 10^9$ [b]	k_1/k_c
$(CH_3)_2CO$	0.807 ± 0.166	2.06	0.391
$(CH_3)_2O$	0.417 ± 0.0906	1.31	0.319
CH_3OH	0.183 ± 0.0408	1.61	0.113
H_2O	0.0341 ± 0.0097	1.96	0.017
$(CH_3)_2NH$	1.43 ± 0.136	1.23	1.16
CH_3NH_2	1.48 ± 0.100	1.44	1.03
NH_3	0.314 ± 0.0348	1.81	0.174

[a] Rate constants are expressed in cm^3 $molecule^{-1}$ s^{-1}.
[b] Calculated according to Ref. [4].

high cooling time to assure the thermalization of the reacting ions; lower cooling time gave rise to semi-log plots with a marked upward curvature which is due to a nonhomogeneous distribution in energy of the ions formed by electron ionization; this suggests that ions with a high energy content form encounter complexes which cannot efficiently dissipate the internal energy before redissociation. According to the reactions depicted in Scheme 1, the disappearance of the ion $C_5H_5M^+$ is a consequence of two competitive reactions, so that this pseudo first order constant is $k_{ps} = b[\text{metallocene}] + c[L]$. Since the pressure of the metallocene was kept constant while the pressure of L was changed within a series of experiments, these pseudo first order constants should exhibit a linear dependence on the ligand pressure. In fact, this was always found. A typical plot is reported in Fig. 1 for the reaction of ammonia with $C_5H_5Ni^+$.

These plots have always an intercept on the y axis, corresponding to the pseudo constant of the reaction of the ion $C_5H_5M^+$ with neutral metallocene. The experimental second order kinetic constants (k_1) obtained from the slopes of these plots are reported in Tables 1–4.

In the same Tables we report the values of the collision rate constants (k_c), evaluated according to the method put forward by Su and Chesnavich [4] along with the reactions efficiencies given by the ratio k_1/k_c. It is apparent that the reaction efficiencies span a large range of values: some reactions are highly efficient, while others are much less so.

It is generally accepted [5] that the overall reaction between an ion and a neutral

$$A^+ + B \rightarrow AB^+$$

can be analysed in terms of the following mechanism:

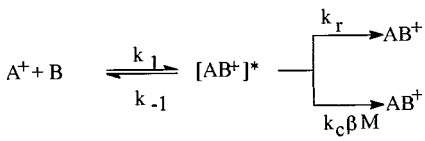

Table 3
Kinetic data for the reactions of the ion $C_5H_5V^+$

Molecule	$k_1 \times 10^9$ [a]	$k_c \times 10^9$ [b]	k_1/k_c
$(CH_3)_2CO$	1.49 ± 0.141	2.08	0.718
$(CH_3)_2O$	1.04 ± 0.193	1.32	0.791
$CH_3CH(OH)CH_3$	1.11 ± 0.220	1.48	0.748
CH_3OH	0.333 ± 0.0410	1.63	0.205
H_2O	0.0150 ± 0.0031	1.96	0.0076
$(CH_3)_3N$	1.31 ± 0.91	1.23	1.06
$(CH_3)_2NH$	0.700 ± 0.172	1.30	0.538
CH_3NH_2	0.597 ± 0.0849	1.49	0.401
NH_3	0.137 ± 0.0410	1.81	0.0756

[a] Rate constants are expressed in cm^3 $molecule^{-1}$ s^{-1}.
[b] Calculated according to Ref. [4].

Table 4
Kinetic data for the reactions of the ion $C_5H_5Ru^+$

Molecule	$k_1 \times 10^9$ [a]	$k_c \times 10^9$ [b]	k_1/k_c
$(CH_3)_2CO$	0.787 ± 0.0524	1.97	0.399
$(CH_3)_2O$	0.621 ± 0.0655	1.26	0.493
$CH_3CH(OH)CH_3$	1.49 ± 0.110	1.40	1.07
CH_3OH	0.0654 ± 0.0089	1.55	0.0421
H_2O	0.00488 ± 0.00061	1.92	0.0025
$(CH_3)_2NH$	1.33 ± 0.0928	1.23	1.08
CH_3NH_2	1.66 ± 0.131	1.44	1.16
NH_3	0.0990 ± 0.0143	1.78	0.0557

[a] Rate constants are expressed in cm^3 $molecule^{-1}$ s^{-1}.
[b] Calculated according to Ref. [4].

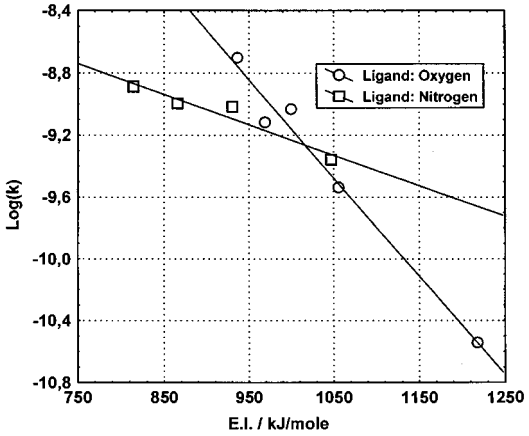

Fig. 2. Rate constants vs. ligand ionization energies for the reactions of $C_5H_5Co^+$.

Table 5
Temperature effect for the reaction of $C_5H_5Fe^+$ with H_2O

Temperature (K)	$k_1 \times 10^{10}$ [a]	$k_c \times 10^{10}$ [b]	k_1/k_c
323	5.23 ± 0.93	21.8	0.240
373	3.54 ± 0.57	20.6	0.175
398	1.85 ± 0.378	20.0	0.092
423	0.23 ± 0.12	19.6	0.012

[a] Rate constants are expressed in cm^3 $molecule^{-1}$ s^{-1}.
[b] Calculated according to Ref. [4].

where: k_1 is the bimolecular rate constant for the collisional complex formation; k_{-1} is the unimolecular redissociation rate constant; k_r is the unimolecular rate constant for the radiative stabilization reaction; k_c is the bimolecular rate constant for collisional stabilization of $[AB^+]^*$ by collision with neutral M and β is the collisional stabilization efficiency. In our system M is the buffer gas He and the ligand L. The He pressure is always much greater then the L pressure (their ratio is usually greater then 100) so that, even if the efficiency of He in the collisional stabilization process is presumably lower then that of L [6], it seems possible to assume that the collision stabilization process is entirely due to He. From the above mechanism, by using the steady state approximation on the intermediate $[AB^+]^*$, the rate of disappearance (v) of the ion A^+ is obtained as

$$v = \frac{k_1 k_c \beta [He][B][A^+]}{k_{-1} + k_c \beta [He] + k_r} + \frac{k_r k_1 [B][A^+]}{k_{-1} + k_c \beta [He] + k_r}$$

Now, at high He pressure (so that $k_c\beta[He] >> k_{-1} + k_r$), the previous equation reduces to

$$v = k_1[A^+][B]$$

so that the observed second order rate constant is simply equal to k_1.

The high He pressure and the long cooling time used in every kinetic run should assure that the saturation limit for the collision stabilization process is reached; this was discussed in Ref. [3] where it was found that any increase of the He pressure beyond 3.5×10^{-2} Pa did not influence the rate constant. During this work occasional checks for this point have been made and it was always found that a decrease of the He pressure and/or the cooling time caused a decrease in the reaction rate while increasing these two parameters has no effect on the reaction rate. The invariance of the observed second order rate constant with the buffer gas pressure has been considered a proof that the high pressure regime has been attained [7–11].

A definite trend can be found in the rate constants. As already found for the association reactions of $C_5H_5Fe^+$ with O- and N-donor ligands, the rate constants increase as the ionization energies of the ligand decrease. Furthermore, it now appears that in some cases the reduction of the ligand ionization energy leads to an efficiency equal to 1 and a further decrease of the ionization energy does not influence the rate constant (see the reactions of $C_5H_5Ni^+$ and $C_5H_5Ru^+$ with the nitrogen donor ligands; for these two ions the reactions with NMe_3 were not studied because it was assumed an efficiency equal to one for their reactions.). Once again the ln of the rate constants is linearly correlated with the ligand ionization energy; a typical plot is shown in the Fig. 2 for the ion $C_5H_5Co^+$. A correlation can also be observed between the ln of the rate constants and the ligand proton affinities; this is not surprising since the proton affinity and the ionization energy are related quantities; slightly better correlation coefficients are however found for the regression lines of the first kind of plots.

An F-test [12] has been carried for the homogeneity of the regression coefficients of these plots. According to this test, the slopes obtained for the oxygen donor ligands can be considered equal regardless of the metals; the same result was found for the nitrogen donor ligands. Therefore, it seems that the above effect is mainly due to the ligand and in particular to the availability of the molecular orbital which is responsible for the first interaction with the $C_5H_5M^+$ ion.

In the ion source of the ITMS only exothermic reactions can be observed and those examined in this study must be of this type, since the interaction of an ion with a polar molecule is attractive in nature. It can be surmised that the low efficiencies found for several reactions are not due to an enthalpy effect. The possibility of an entropy effect on the reactions can be considered. To elucidate this particular aspect, some of the above reactions were performed at various temperatures. The results are reported in Tables 5–7 along with the reaction efficiencies.

The data reported in these last Tables indicate an anti-Arrhenius behaviour, with the rate constants increasing when the temperature is decreasing. This kind of rate constant dependence on the temperature is frequently found in gaseous phase ion molecule association reactions but it was found only in the low pressure regime [7,8,13]. In this case, the overall association rate constant contains the equilibrium constant between reactants and the excited complex, and the temperature effect on the overall rate constant is mainly due to the effect on the equilibrium constant. However, as previously noted, our data are taken under the condition of the high pressure limit, so that the above explanation should not hold. The data seem to indicate the possibility of a limiting value for the reaction efficiency at low temperature. The plot of $\ln(k_1/k_c)$ versus T reported in Fig. 3 for the reaction of $C_5H_5Fe^+$ with methanol seems significant to this regard.

Table 6
Temperature effect for the reaction of $C_5H_5Fe^+$ with CH_3OH

Temperature (K)	$k_1 \times 10^{9}$ [a]	$k_c \times 10^{9}$ [b]	k_1/k_c
323	1.56 ± 0.266	1.77	0.881
348	1.56 ± 0.160	1.73	0.901
373	1.25 ± 0.171	1.69	0.737
398	0.756 ± 0.0836	1.65	0.457
423	0.296 ± 0.0286	1.62	0.183
473	0.129 ± 0.0314	1.56	0.0826

[a] Rate constants are expressed in cm^3 $molecule^{-1}$ s^{-1}.
[b] Calculated according to Ref. [4].

Table 7
Temperature effect for the reaction of $C_5H_5Ru^+$ with CH_3OH

Temperature (K)	$k_1 \times 10^{10}$ [a]	$k_c \times 10^{10}$ [b]	k_1/k_c
323	3.95 ± 0.373	17.0	0.232
373	2.86 ± 0.305	16.2	0.176
423	0.654 ± 0.089	15.5	0.0421
473	0.341 ± 0.0739	14.9	0.0228

[a] Rate constants are expressed in cm^3 $molecule^{-1}$ s^{-1}.
[b] Calculated according to Ref. [4].

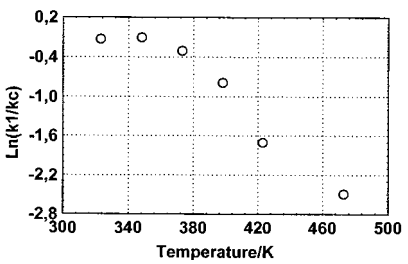

Fig. 3. $\mathrm{Ln}(k_1/k_c)$ vs. temperature for the reaction of $C_5H_5Fe^+$ with methanol.

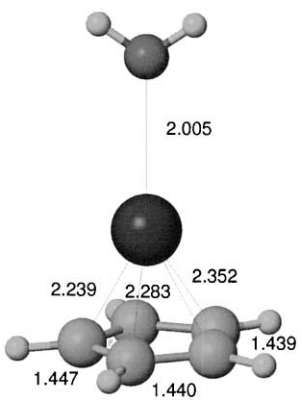

Fig. 4. The DFT(B3LYP)/LANL2DZ optimized structure of the complex between water and $FeCp^+$. The main interatomic distances are reported in angstrom.

This trend recalls that reported by Bohme et al. [14] and more recently by Bouchoux et al. [15] for proton transfer reactions. In those papers a high efficiency for highly exoergic proton transfer is reported but the efficiency decreases as the proton transfer approaches thermoneutrality; and a linear relationship was found between the ln of the reaction efficiency and the reaction free energy variation for moderately endoergic reactions. The reaction entropy variation should be negative for the reactions studied in this paper. Therefore, the free energy variation of the reaction should become less negative as the temperature increases. However a low reaction efficiency is expected only for slightly exoergic reactions ($\Delta G^{\ddagger} < -20$ kJ mol^{-1}) but the high exothermicity of the present association reactions should prevent the possibility that the reaction free energy variation approaches to zero, suggesting that this model is not applicable to the present results.

In the attempt of gaining a sounder explanation for the present experimental results we resorted to perform some calculations on the simplest system: the reaction of water with $C_5H_5Fe^+$. The study of the $H_2O + FeC_5H_5^+$ reaction was begun by determining, on the reaction energy hyper-surface, the critical points corresponding to the $FeC_5H_5^+$ and H_2O–$FeC_5H_5^+$ structures (Fig. 4; the more important optimum interatomic distances are reported in ångströms).

Calculations were carried out with the spin multiplicities 1, 3, and 5. The quintet results to be the more stable spin state, being 43.9 or 66.9 kJ mol^{-1} lower than the triplet, for $FeC_5H_5^+$ and H_2O–$FeC_5H_5^+$, respectively. The triplet is in turn 88.3 or 74.5 kJ mol^{-1} more stable than the singlet, again in the $FeC_5H_5^+$ and H_2O–$FeC_5H_5^+$ cases. (In the naked Fe^{++} ion these differences are significantly larger, the quintuplet being more stable than the triplet by 249 kJ mol^{-1}, and the triplet 653 kJ mol^{-1} more stable than the singlet). The complexation reaction is quite exoergic, by 225.5 kJ mol^{-1} for the quintet multiplicity (by 202.5 and 216.7 for the triplet and singlet multiplicities, respectively). Only the quintet energy profile was studied further. No

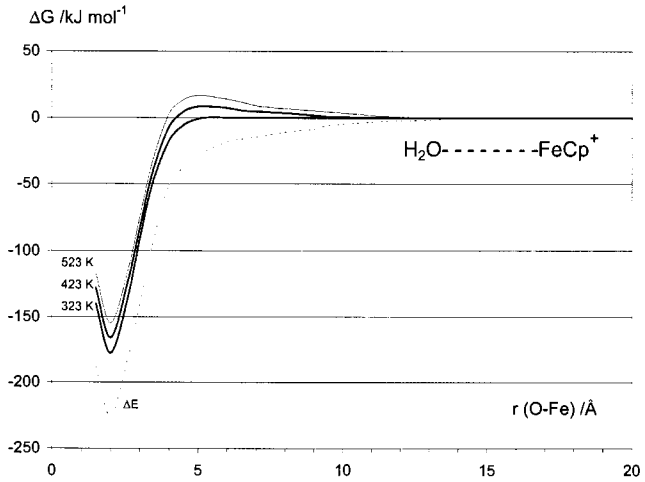

Fig. 5. The energy (dashed line) and free energy (solid lines) profiles for the association of H_2O and $FeCp^+$. Three free energy profiles corresponding to different temperatures are displayed: two of them (thick lines) can be compared with the experiments discussed in the text, the third one (thin line) is just computed.

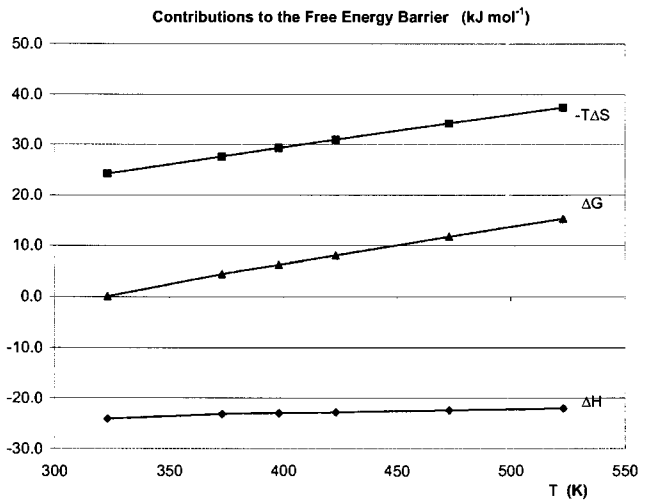

Fig. 6. Contributions from the $\Delta H^{\ddagger}$ (diamonds) and $-T\Delta S^{\ddagger}$ (squares) terms to the free energy barrier $\Delta G^{\ddagger}$ (triangles) for the association of H_2O and $FeCp^+$, reported for temperatures ranging from 323 to 523 K.

transition structure, along the complexation pathway of the two molecules, was detected on that energy hypersurface. Therefore, in order to obtain an approximate reaction profile (Fig. 5) some additional points were determined in correspondence to selected interfragment O–Fe distances, by optimizing all the other geometrical parameters.

For all stable structures, a vibrational analysis was carried out, in order to estimate the enthalpy, the entropy contributions, and to get an approximate free energy profile. The imaginary frequency corresponding to the reaction coordinate was discarded in computing the vibrational contribution to the entropy. Some oscillations in the frequency values of important low-frequency vibrations occurred in correspondence to the O–Fe distance range 7–9 Å. Obviously, these disturbing fluctuations bring about corresponding variations in the vibrational contributions to the entropy for the relevant modes. This problem was addressed by Baboul and Schlegel [16], who suggested to define very accurately the optimum geometry along the reaction path in order to avoid such fluctuations. Unfortunately very long optimization runs were unaffordable to us with this system. Therefore, considering that the points in the distance range mentioned are probably of limited interest, we preferred to eliminate these data.

The complexation exothermicity is reduced by a temperature increase, as shown in Fig. 6.

The overall entropy change, in going from the separated moieties to the complex, is -112.5 J mol^{-1} K^{-1} at $T = 323$ K, or -110.9 J mol^{-1} K^{-1} at $T = 423$ K, showing a small implicit dependence on T. But the reaction ΔG changes more significantly, from -177.8 to -165.7 kJ mol^{-1}, obviously due to the direct dependence on T of the entropic term. This explicit dependence dictates also the change in ΔG of activation as a function of the temperature, and is significant enough to introduce some free-energy overhead on the reaction profile. A modest hump is thus present in the G profile, ca. 8–12 kJ mol^{-1} high with respect to the dissociation limit. It occurs in correspondence to a O–Fe distance of 5.5 Å (the optimum O–Fe distance in the complex is 2.0 Å). In Table 8 the enthalpy, entropy, and free energy at an O–Fe distance of 5.5 Å are collected, in correspondence to six different temperatures. Even if the results of these calculations should be considered only qualitative in nature, they point in the direction of an entropy effect on the reaction efficiency.

Table 8
Enthalpy, entropy, and free energy differences at a distance $r_{OFe} = 5.5$ Å, relative to the separated H_2O and $FeCp^+$ moieties

Temperature (K)	ΔH (kJ mol^{-1})	$-\Delta S$ (J mol^{-1} K^{-1})	$-T\Delta S$ (kJ mol^{-1})	ΔG (kJ mol^{-1})
323	−24.18	0.075	24.24	0.04
373	−23.22	0.074	27.63	4.40
398	−23.04	0.073	29.29	6.25
423	−22.86	0.073	30.95	8.08
473	−22.49	0.072	34.21	11.72
523	−22.10	0.071	37.42	15.32

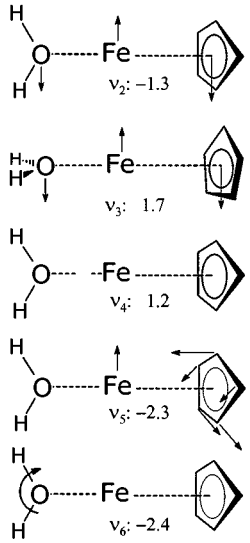

Fig. 7. Pictorial representation of the most prominent vibrational contributions to the entropy change in going from the separate reactants to the oxygen–iron distance of 5.5 Å. Each number associated to a vibrational mode represents a contribution to ΔS (in cal mol^{-1} K^{-1}).

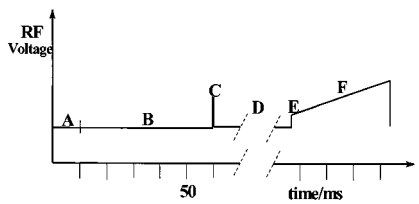

Fig. 8. Scan function used to obtain the kinetic data: (A) ionization; (B) cooling time; (C) isolation step; (D) reaction time; (E) scan start; (F) spectrum acquisition.

In Fig. 7 the most important vibrational contributions to the entropy change that occurs when the two moieties are brought together (from a large O–Fe distance to ca. 5.5 Å) are displayed. The overall vibrational contribution to the estimated $\Delta S^{\ddagger}$ is -11.7 j mol^{-1} K^{-1}. It must be observed, however, that the rotational contribution is ca. -32.2 j mol^{-1} K^{-1}.

According to this hypothesis the reaction efficiency depends on the reaction thermodynamics. There are two factors which govern the free activation energy: the reaction exothermicity and the entropy of activation; these two factors act in opposition each other; since the entropy effect is rather small it can be observed only with the less exothermic reactions. The existing data on the C_5H_5M–L^+ bond dissociation energies are not extensive. However, data are available [17] for the $C_5H_5Ni^+$ ion, which show that the bond dissociation energy increases on going from ammonia to the methylamines and that the bond dissociation energies of the oxygen donor ligands are lower than those of the nitrogen donor ligands. The exothermicity of the addition reactions should parallel the trend of the bond dissociation energies.

In this way the variation of the reaction efficiency in the reactions of the $C_5H_5Ni^+$ ion can be explained since the ligands with lower ionization energy are those with a more pronounced well in the energy profile of the reaction and in these cases the entropy effect is not able to make positive the overall free activation energy.

In addition, it is very likely that the order found for the $C_5H_5Ni^+$ ion holds also for the other ions, since in several metal ion systems the order of the M–L^+ binding energy is the same [18–23]. Thus, the above effect should hold for all the reactions studied so affording a qualitative explanation of the results. Entropy effects have recently [24–28] used in assessing thermodynamic quantities obtained by the kinetic method but to our knowledge they have not been previously invoked in connection with the low efficiencies often found in gas phase ion molecule reactions. The present results are however in line with the many studies on gaseous phase radical reactions; in these reactions, which proceed with very low or zero activation energy, anti-Arrhenius behaviour [29–32] as well as negative activation entropy [33–35] are often found. In effect negative activation energy is usually taken as a proof of an association rate determining [31] step also in reactions involving some bond breaking; however, since this kind of reactions are more commonly studied in the low pressure region, this behaviour is usually related to an effect on the equilibrium constant [36] for the association step. We feel to have now given evidence of a direct effect of the activation entropy on the reaction rate constant.

3. Experimental

Measurements have been done with a Finnigan Ion Trap Mass Spectrometer (ITMS). The general procedure to obtain kinetic data is as follows. The metallocenes are introduced in the ion trap via the direct insertion probe, while helium and the ligand (L) are introduced in the mass spectrometer via two different standard gas inlet devices. The metallocene pressure was usually around 8×10^{-5} Pa, the He pressure was kept constant at 3.5×10^{-2} Pa. The pressure of the ligands changed between about 7×10^{-6} and 3×10^{-4} Pa. The effective range for each ligand being determined by the reaction rate. The ion $C_5H_5M^+$ is formed by electron ionization with an ionization time of 10 ms at a starting $m/z = 100$; in this way ions of lower mass are ejected from the ion source. The ion is then cooled for 50 ms and, after the isolation with the apex technique [37], several spectra are acquired at different reaction times. The scan function is shown in Fig. 8.

The reaction time is changed by software. Usually two spectra are collected at each reaction time for a total of 26–30 spectra in a time range sufficient to

reduce the relative intensity of the ion $C_5H_5M^+$ from 100% to about 10–5%. The relative intensity of this last ion was calculated with respect to the total ion intensities. In the adopted experimental conditions the ligand pressure, in a single kinetic run, is constant so that the disappearance of the ion $C_5H_5M^+$ must follow first order kinetics. From the plots of the ln of its relative intensity versus reaction time the pseudo first order rate constants can be obtained.

The gas pressure was monitored with a Bayard–Alpert gauge; the corrections for the different gauge sensitivity have been made by using literature ionization cross sections when available [38–40]. In the absence of these data, as in the case of trimethyl- and dimethylamine, the ionization cross section has been estimated by using the relation between the polarizability and the cross section [39] and the postulate of atomic cross section additivity [41]. In this last case a fair agreement was found between the two calculated values. Kinetic data have been checked for homogeneity by using the F-test; reported uncertainties in the Tables are the standard errors [42]; those last values indicate the high reproducibility of the measurements while the precision of the kinetic constant values strongly depend upon the pressure measurements and an uncertainty of about 25% is reasonable for the kinetic constants.

3.1. Theoretical method

Density functional theory (DFT) [43] was used throughout, in conjunction with the hybrid exchange-correlation functional made up by the three-term exchange functional propounded by Becke (B3) [44], and by the correlation functional of Lee, Yang, and Parr (LYP) [45]. The study of the $H_2O + FeCp^+$ reaction was performed by determining, on the reaction energy hypersurface, the critical points corresponding to the $FeCp^+$ and H_2O–$FeCp^+$ structures. No transition structure for the association of the two moieties was found. To obtain an approximate reaction energy profile, some extra points were defined in correspondence to fixed interfragment O–Fe distances, by unconstrained optimizations in the subspace of the remaining parameters. All these structures were fully optimized by gradient procedures [46] at the DFT(B3LYP) theory level, using the LANL2DZ basis set [47]. This is made up by a double-ζ Huzinaga–Dunning gaussian basis set [47a] on the C, O, and H atoms, while on Fe it contains effective core potentials with relativistic terms for the inner electrons, and a double-ζ basis for the outer electrons, whereas the outermost core orbitals are explicitly introduced through a double-ζ basis, as the valence electrons [47b]. For the stable structures and the additional structures at fixed O–Fe distances, a vibrational analysis was carried out, in order to estimate the entropy contributions and the free energy profile. All calculations were carried out using the GAUSSIAN-98 system of programs [48].

Acknowledgements

The authors gratefully acknowledge the financial support to this work provided by the University of Torino, the University of Bologna, and the MURST (Cofinanziamento 1997, national project 'Reattività e Struttura di Specie Ioniche in Fase Gassosa'). Fig. 4 was drawn with MolMol 2.4 [49].

References

[1] D. Ekeberg, E. Uggerud, H. Lin, K. Sohlberg, H. Chen, D.P. Ridge, Organometallics 18 (1999) 40.
[2] P.A.M. van Koppen, M.T. Bowers, E.R. Fisher, P.B. Armentrout, J. Am. Chem. Soc. 116 (1999) 3780.
[3] G. Innorta, L. Pontoni, S. Torroni, J. Am. Chem. Soc. Mass Spectrom 9 (1998) 314.
[4] T. Su, W.J. Chesnavich, J. Chem. Phys. 76 (1982) 5183.
[5] V. Ryzhov, S.J. Klippenstein, R. Dumbar, J. Am. Chem. Soc. 118 (1996) 5462.
[6] D. Gerlich, S. Horning, Chem. Rev. 92 (1992) 1509.
[7] M. Meot-Ner, F.H. Field, J. Am. Chem. Soc 97 (1975) 5339.
[8] D. Smith, N.G. Adams, Chem. Phys. Lett. 54 (1978) 535.
[9] W.N. Olmstead, M. Lev-On, D.M. Golden, J.I. Brauman, J. Am. Chem. Soc. 99 (1977) 992.
[10] P. Kofel, T.B. McMahon, J. Phys. Chem. 92 (1988) 6174.
[11] S.J. Klippenstein, Yu-C. Yang, V. Ryzhov, R.C. Dunbar, J. Chem. Phys. 104 (1996) 4502.
[12] R.G.D. Steel, J.H. Torrie, Principles and Procedures of Statistics, McGraw-Hill, New York, 1960, p. 319.
[13] A.A. Viggiano, J. Chem. Phys. 84 (1986) 244 and references therein.
[14] D.K. Bohme, G.I. Mcakay, H.I. Schiff, J. Chem. Phys. 73 (1980) 4976.
[15] G. Bouchoux, J.Y. Salpin, D. Leblanc, Int. J. Mass Spectrom. Ion Processes 153 (1996) 37.
[16] A.G. Baboul, H.B. Schlegel, J. Chem. Phys. 107 (1997) 9413–9417.
[17] J.A.M. Simoes, J.L. Beauchamp, Chem. Rev. 90 (1990) 629.
[18] R.R. Cordeman, J.L. Beauchamp, J. Am. Chem. Soc. 98 (1976) 3998.
[19] M.S. El-Shall, K.E. Schriver, R.L. Whetten, M. Meot-Ner, J. Phys. Chem. 93 (1989) 7969.
[20] L. Operti, E.C. Tews, B.S. Freiser, J. Am. Chem. Soc. 110 (1988) 3847.
[21] J.S. Uppal, R.H. Staley, J. Am. Chem. Soc. 104 (1982) 1238.
[22] R.W. Jones, R.H. Staley, J. Am. Chem. Soc. 104 (1982) 2296.
[23] J.S. Uppal, R.H. Staley, J. Am. Chem. Soc. 104 (1982) 1235.
[24] X. Cheng, Z. Wu, C.J. Fenselau, J. Am. Chem. Soc. 115 (1993) 4844.
[25] B.A. Cerda, C. Wesdemiotis, J. Am. Chem. Soc. 118 (1996) 11884.
[26] K.K. Irikura, J. Am. Chem. Soc. 121 (1999) 7689.
[27] P.B. Armentrout, J. Am. Soc. Mass Spectrom. 11 (2000) 371.
[28] P.G. Wenthold, J. Am. Soc. Mass Spectrom. 11 (2000) 601.
[29] C. Fittschen, A. Frenzel, K. Imrik, P. Devolle, Int. J. Chem. Kinet. 31 (1999) 860.

[30] M.K. Gilles, J.B. Burkholder, A.R. Ravishankara, Int. J. Chem. Kinet. 31 (1999) 417.
[31] M.A.E. Edwards, J.F. Hershberger, Chem. Phys 234 (1998) 231.
[32] J. Le Calvè, D. Hitier, G. Le Bras, A. Mellouki, J. Phys. Chem. Sect. A 102 (1988) 4579.
[33] A. Shepp, K.O. Kutschke, J. Chem. Phys. 26 (1957) 1020.
[34] A.C. Olleta, R.A. Taccone, J. Mol. Struct. 507 (2000) 25.
[35] P. Sainte Claire, H. Peslherbe, H. Wang, W.L. Hase, J. Am. Chem. Soc. 119 (1997) 5007.
[36] S.W. Benson, Thermochemical Kinetics, Wiley, New York, 1968.
[37] M. Weber-Grabau, P.E. Kelley, J.E.P. Syka, S.C. Bradshaw, J.S. Brodelbet, Proceedings of the 35th ASMS Conference on Mass Spectrometry and Allied Topics, Denver, CO, 1987, p 1114.
[38] A.G. Harrison, E.G. Jones, S.K. Gupta, G.P. Nagy, Can. J. Chem. 44 (1966) 1967.
[39] F.W. Lampe, J.L. Franklin, F.H. Field, J. Am. Chem. Soc. 79 (1957) 6129.
[40] H.J. Grosse, H.K. Bothe, Z. Naturforsch. 23a (1968) 1583.
[41] J.W. Otvos, D.P. Stevenson, J. Am. Chem. Soc 78 (1956) 546.
[42] D. Margerison, in: C.H. Banford, C.F.H. Tipper (Eds.), Comprehensive Chemical Kinetics, vol. 1, Elsevier, 1969, p. 343.
[43] R.G. Parr, W. Yang, Density Functional Theory of Atoms and Molecules, Oxford University Press, New York, 1989, p. 3.
[44] (a) A.D. Becke, Phys. Rev. Sect. A 38 (1988) 3098. (b) A.D. Becke, ACS Symp. Ser. 394 (1989) 165. (c) A.D. Becke, J. Chem. Phys. 98 (1993) 5648.
[45] C. Lee, W. Yang, R.G. Parr, Phys. Rev. Sect. B 37 (1988) 785–789.
[46] J.A. Pople, P.M.W. Gill, B.G. Johnson, Chem. Phys. Lett. 199 (1992) 557.
[47] (a) T.H. Dunning Jr., P.J. Hay, Modern Theoretical Chemistry, vol. 3, in: H.F. Schafer (Ed.), chapter 1, Plenum Press, New York, 1976. (b) P.J. Hay, W.R. Wadt, J. Chem. Phys. 82 (1985) 299.
[48] GAUSSIAN-98, Revision A.6. M.J. Frisch, G.W. Trucks, H.B. Schlegel, G.E. Scuseria, M.A. Robb, J.R. Cheeseman, V.G. Zakrzewski, J.A. Montgomery, Jr., R.E. Stratmann, J.C. Burant, S. Dapprich, J.M. Millam, A.D. Daniels, K.N. Kudin, M.C. Strain, O. Farkas, J. Tomasi, V. Barone, M. Cossi, R. Cammi, B. Mennucci, C. Pomelli, C. Adamo, S. Clifford, J. Ochterski, G.A. Petersson, P.Y. Ayala, Q. Cui, K. Morokuma, D.K. Malick, A.D. Rabuck, K. Raghavachari, J.B. Foresman, J. Cioslowski, J.V. Ortiz, B.B. Stefanov, G. Liu, A. Liashenko, P. Piskorz, I. Komaromi, R. Gomperts, R.L. Martin, D.J. Fox, T. Keith, M.A. Al-Laham, C.Y. Peng, A. Nanayakkara, C. Gonzalez, M. Challacombe, P.M.W. Gill, B. Johnson, W. Chen, M.W. Wong, J.L. Andres, C. Gonzalez, M. Head-Gordon, E.S. Replogle, and J.A. Pople, Gaussian Inc., Pittsburgh PA, 1998.
[49] MolMol 2.4. A graphic program developed by the Institut für Molekular-biologie und Biophysik, EHT Zurich Spectrospin AG, Faellenden, Switzerland, R. Koradi, M. Billeter, K. Wüthrich, J. Mol. Graphics 14 (1996) 51.